frontiers | Frontiers in Electronic Materials

TYPE Mini Review
PUBLISHED 06 February 2025
DOI 10.3389/femat.2025.1456147

OPEN ACCESS

EDITED BY
Umesh Kumar,
The State University of New Jersey,
United States

REVIEWED BY
Kenji Ishii,
National Institutes for Quantum Science and Technology, Japan
Nitin Kaushal,
University of British Columbia, Canada

*CORRESPONDENCE
Takashi Mizokawa,
mizokawa@waseda.jp

RECEIVED 28 June 2024
ACCEPTED 15 January 2025
PUBLISHED 06 February 2025

CITATION
Mizokawa T and Monney C (2025) Excitonic insulator candidate Ta_2NiSe_5 and related transition-metal compounds studied by resonant inelastic x-ray scattering.
Front. Electron. Mater. 5:1456147.
doi: 10.3389/femat.2025.1456147

Excitonic insulator candidate Ta_2NiSe_5 and related transition-metal compounds studied by resonant inelastic x-ray scattering

Takashi Mizokawa[1]* and Claude Monney[2]

[1]Department of Applied Physics, Waseda University, Tokyo, Japan, [2]Département de Physique and Fribourg Center for Nanomaterials, Université de Fribourg, Fribourg, Switzerland

Resonant inelastic x-ray scattering (RIXS) can probe electron-hole excitations in excitonic insulators (EIs) which are realized by Coulomb attractive interaction between electrons and holes in semimetals or narrow gap semiconductors. In the present article, we review the exotic electronic state of an EI candidate Ta_2NiSe_5 which is probed by Ni 2p-3d RIXS as well as Ni 2p x-ray photoemission/absorption spectroscopy. The RIXS results on the exotic electronic state under the electron-hole and electron-lattice correlations suggest requirement of a new theoretical scheme which can describe itinerant electron-hole excitations and the localized charge-transfer excitations as well as the electron-lattice interaction.

KEYWORDS

resonant inelastic x-ray scattering (RIXS), excitonic insulator candidate, transition-metal chalcogenides, negative charge-transfer energy, electron-hole excitations

1 Introduction to excitonic insulators and a layered chalcogenide Ta_2NiSe_5

In narrow gap semiconductors or semimetals, the attractive Coulomb force between electrons and holes can induce an excitonic insulator (EI) ground state when the band gap energy, E_G is smaller than the electron-hole binding energy. A canonical phase diagram is illustrated in Figure 1A. The EI phase appears in between the semiconductor phase ($E_G > 0$) and the semimetal phase ($E_G < 0$). The phase transition to the EI state can be viewed as a Bose-Einstein condensation of electron-hole pairs. As shown in Figure 1B, the attractive Coulomb force between electrons and holes creates a band gap at the Fermi level in the EI phase. The pioneering theories in 1960s (Mott, 1961; Jerome et al., 1967; Zittartz, 1967; Halperin and Rice, 1968) were followed by more detailed theoretical works revealing BCS-BEC crossover from the semimetal side to the semiconductor side of the phase diagram (Bronold and Fehske, 2006; Bronold and Fehske, 2006; Ihle et al., 2008; Phan et al., 2010).

In spite of the theoretical achievements, experimental studies on EIs have been limited to a few materials such as Tm(Se,Te) (Neuenschwander and Wachter, 1990; Bucher et al., 1991; Wachter et al., 2004). EI nature of Tm(Se,Te) is not well established partly due to its magnetism. $TiSe_2$ is known to exhibit a charge density wave (DiSalvo et al., 1976). The origin of the charge density wave has been investigated by angle-resolved photoemission spectroscopy (ARPES) (Pillo et al., 2000; Rossnagel et al., 2002; Qian et al., 2007; Zhao et al., 2007). While the importance of electron-lattice interaction was emphasized in the early

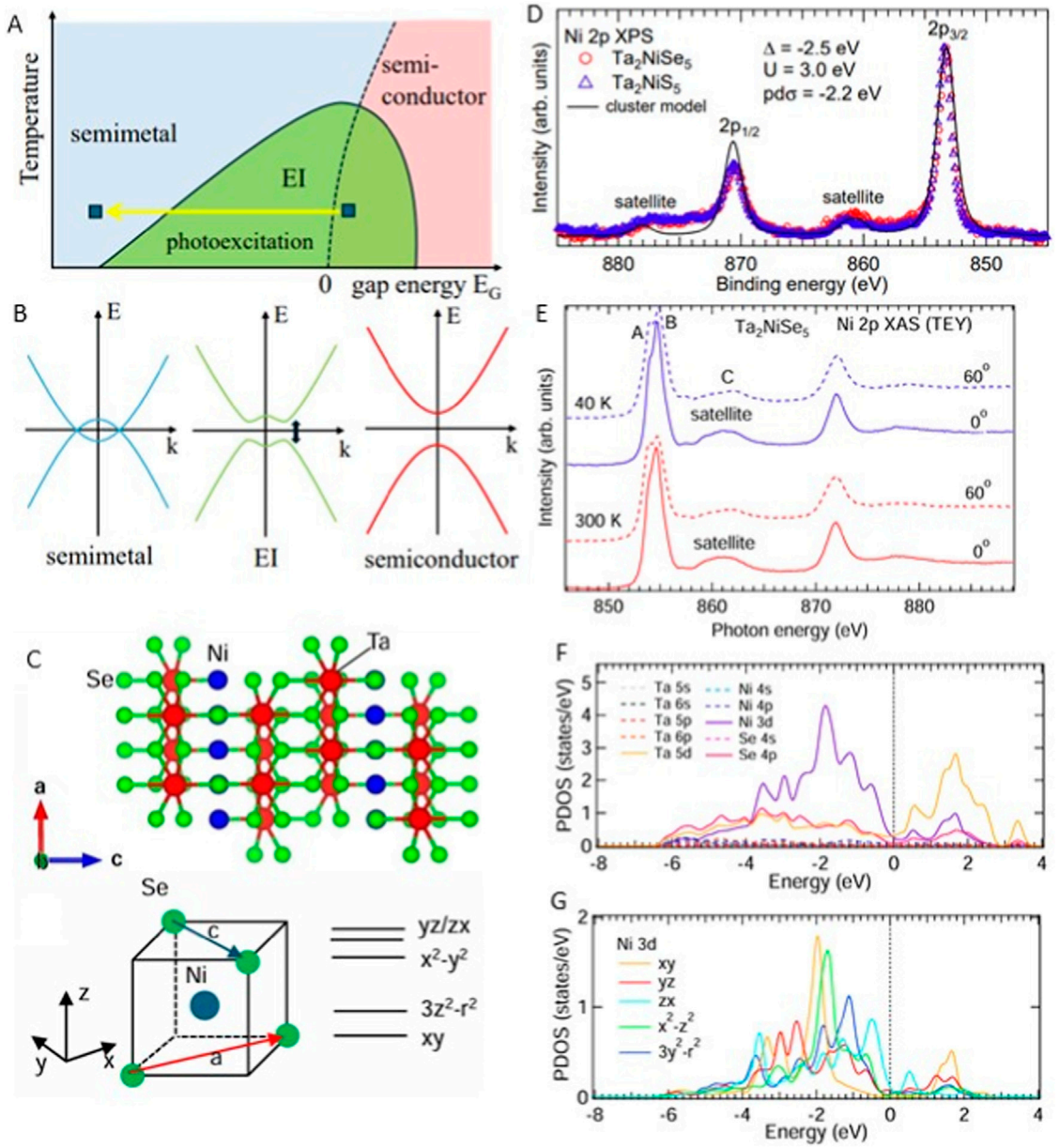

FIGURE 1
(A) Canonical phase diagram of EIs as a function of band gap energy, E_G and temperature T. The arrow indicates a photo-induced phase transition from the EI state to the semimetal states **(B)** Typical band structure for the semimetal, EI, and semiconductor states. **(C)** Crystal structure of Ta_2NiSe_5 in the a-c plane and $NiSe_4$ tetrahedron with the ligand field splitting of the Ni 3d orbitals. Ni chains run along the a-axis. **(D)** Ni 2p XPS spectra of Ta_2NiSe_5 and Ta_2NiS_5 reproduced from the literature (Chiba et al., 2019). The solid curve represents a theoretical spectrum calculated by a $NiSe_4$ cluster model. **(E)** Ni 2p XAS spectra of Ta_2NiSe_5 taken by TEY with linearly polarized x-ray of normal incidence (0°) and grazing incidence (60°). **(F)** Ta, Ni, and Se PDOS calculated by GGA for Ta_2NiSe_5 reproduced from the literature (Takahashi and Mizokawa, 2022). **(G)** Ni 3d orbital-resolved PDOS by GGA.

stage, the EI scenario of the charge density wave has been proposed based on ARPES results of $TiSe_2$ (Pillo et al., 2000; Cercellier et al., 2007; Monney et al., 2009; Monney et al., 2010). The nature of the electron-hole excitations has been revealed by ARPES (Monney et al., 2012a), electron energy loss spectroscopy (Kogar et al., 2017), and resonant inelastic x-ray scattering (RIXS) (Monney et al., 2012b). The optical control of the band folding and the band gap has been achieved by time-resolved ARPES (Rohwer et al., 2011; Monney et al., 2016; Huber et al., 2024) and time-resolved RIXS (Lu et al., 2020).

In real materials, EI states are accompanied by various structural distortions since the symmetry broken electronic states can be stabilized further by electron-lattice interaction. In the case of $TiSe_2$, the possible EI phase exhibits the 2 × 2 × 2 superstructure corresponding to the momentum transfer between the valence band top at Γ point and the conduction band bottom at L point in the hexagonal Brillouin zone. A layered transition-metal chalcogenide Ta_2NiSe_5, in which tetrahedrally coordinated Ni sites and octahedrally coordinated Ta sites form chains along the a-axis (see Figure 1C), undergoes structural phase transition from

orthorhombic to monoclinic around 328 K (Sunshine and Ibers, 1985; DiSalvo et al., 1986; Canadell and Whangbo, 1987) which is proposed to be a transition to the EI state by ARPES (Wakisaka et al., 2009; Wakisaka et al., 2012) and by theoretical calculations (Seki et al., 2011; Kaneko et al., 2013). The valence band top and the conduction band bottom are located at Γ point in Ta_2NiSe_5 as well as in Ta_2NiS_5. Among the EI candidates, Ta_2NiSe_5 without superstructure and magnetism provides an ideal platform to study a possible EI state by means of various experimental and theoretical techniques. The electron-hole fluctuations above the transition temperature have been revealed by comparison between ARPES and calculations beyond mean field approximation (Seki et al., 2014). The pseudogap behavior above the transition temperature (Seki et al., 2014) suggests that the possible EI state falls in the BEC regime of the BCS-BEC crossover (Ejima et al., 2014). S substitution for Se and physical pressure can control E_G and the transition temperature, and their variations are consistent with the phase diagram of EIs (Lu et al., 2017). On the other hand, optical measurements have revealed importance of electron-lattice interaction (Larkin et al., 2017; Larkin et al., 2018; Werdehausen et al., 2018). The monoclinic distortion and the band gap can be suppressed by pressure (Nakano et al., 2018), and Ta_2NiSe_5 exhibits pressure-induced superconductivity at low temperatures (Matsubayashi et al., 2021). The existence of the lattice distortion indicates that the possible EI state of Ta_2NiSe_5 falls in the q = 0 charge-density wave class among the four classes of EI states (charge-density wave, charge-current-density wave, spin-density wave, and spin-current-density wave) (Halperin and Rice 1968). It would be interesting to note that the spin-current-density wave class was proposed for $NiGa_2S_4$ based on ARPES (Takubo et al., 2010). When the EI states are formed purely by the electron-hole Coulomb interaction, their charge excitations are characterized by the gapped amplitude mode and the gapless phase mode (Kogar et al., 2017). In Ta_2NiSe_5, the q = 0 charge-density wave state is accompanied by the monoclinic distortion, indicating that the phase mode excitation is gapped and mixed with phonon excitations (Murakami et al., 2020). Even though the phase of the order parameter is locked by the lattice distortion, the band gap in the single-particle excitation and the amplitude mode gap in the charge excitation may exhibit interesting optical response. Indeed, the band gap of Ta_2NiSe_5 can be enhanced (Mor et al., 2017) or can be destroyed (Okazaki et al., 2018) by optical excitations with the 100 fs time scale while the nonthermal structural transition is inhibited (Mor et al., 2018). The dynamics of the electron-hole pairs governs the photoinduced phase transition to a semimetal state and the subsequent recovery of the insulating state (Okazaki et al., 2018). In the exotic electronic state with the monoclinic distortion, it is likely that the charge gap is mainly created by the electron-hole interaction. In the current research activities, such a situation is frequently denoted as a "EI state" in a broad sense even though the phase mode is gapped. The band structure of the monoclinic phase in Ta_2NiSe_5 and $Ta_2Ni(Se_{1-x}S_x)_5$ is probed by ARPES (Lee et al., 2019; Fukutani et al., 2019; Watson et al., 2020; Mazza et al., 2020; Fukutani et al., 2021; Hattori et al., 2023) while the excitations across the band gap can be observed by scanning tunnelling spectroscopy (He et al., 2021) and optical spectroscopy (Volkov et al., 2021; Ye et al., 2021; Okamura et al., 2023). The unoccupied part of the band structure was studied using two-photon-photoemission spectroscopy (Mor et al., 2022). However, a drastic photo-induced phase transition from the insulating state to a nodal-line semimetal state was probed (Okazaki et al., 2018) using time-resolved ARPES at high fluence supporting the EI scenario. The details of the photo-induced phase transition have been revealed by transient optical spectroscopy (Kim et al., 2021; Bretscher et al., 2021; Miyamoto et al., 2022) and time-resolved ARPES (Mitsuoka et al., 2020; Liu et al., 2021; Saha et al., 2021; Suzuki et al., 2021; Takahashi et al., 2023; Baldini et al., 2023). In particular, in the result by Baldini et al., Ta_2NiSe_5 did not show the photo-induced semimetal state suggesting that the band gap is created by the monoclinic lattice distortion. The different behaviours against the photo-excitations are not fully understood yet. The interplay between the electron-hole interaction and the electron-phonon interaction has been elucidated by the recent pump-probe optical measurements (Haque et al., 2024; Jiang et al., 2024). A more recent EI candidate $Ta_2Pd_3Te_5$ (Zhang et al., 2024; Huang et al., 2024) is accompanied by a relatively small lattice distortion. The relationship between the optical response of the band gap and the lattice distortion should be studied in a systematic manner in the EI candidate materials. The difference between Ta_2NiSe_5 and $Ta_2Pd_3Te_5$ may indicate importance of the more localized character of Ni 3d states providing stronger electron-lattice interaction.

The unoccupied part of the band structure in the possible EI phase can also be observed by angle-resolved resonant inelastic x-ray scattering (RIXS) at the Ni 2p-3d absorption edge of Ta_2NiSe_5 (Monney et al., 2020). When the interaction between the core hole and the excited electron is strong enough, the RIXS spectra can be interpreted as charge/orbital/spin excitations of the localized electrons (Kotani and Shin, 2001; Ament et al., 2011). In various 3d transition-metal oxides with partially filled 3d subshell, the RIXS spectra at transition-metal 2p to 3d excitations are usually interpreted using localized models such as the NiO_6 cluster model for NiO and the $NiSe_4$ cluster model illustrated in Figure 1C for the title system. In case of Ta_2NiSe_5, the Ni 3d orbitals are almost fully occupied, and the interaction between the Ni 2p core hole and the conduction band electron is rather weak (Monney et al., 2020). In this situation, the RIXS spectra can be interpreted by the electron-hole excitations between the valence and conduction bands as first proposed by Monney et al. for $TiSe_2$ (Monney et al., 2012b). Here, it should be noted that the electron-hole Coulomb interaction creates the band gap of the single-particle excitation (or the amplitude mode gap of the charge excitation) in canonical EIs. The electron-lattice interaction also contributes to create the band gap. In the case of Ta_2NiSe_5, the photoinduced semimetal state with the monoclinic distortion indicates importance of the electron-hole Coulomb interaction. Please note that the electron-hole excitations across the amplitude mode gap are different from the excitons.

In the present contribution, RIXS studies on the EI candidates including Ta_2NiSe_5 are reviewed with theoretical overviews. After the brief introductory description of EI candidates in Section 1, x-ray photoemission spectroscopy (XPS) and x-ray absorption spectroscopy (XAS) of Ni 2p core level in Ta_2NiSe_5 will be reviewed in Section 2. In Section 3, angle-resolved RIXS results on Ta_2NiSe_5 will be reviewed to discuss electron-hole excitations

across the band gap. The XAS, XES, and RIXS results suggest that Ta_2NiSe_5 deviates from the canonical EI state through the involvement of the localized Se 4p-Ni 3d charge-transfer excitation.

2 X-ray spectroscopy (XPS, XAS, XES) of Ta_2NiSe_5

Figure 1D shows Ni 2p XPS spectra of Ta_2NiSe_5 and Ta_2NiS_5 taken at room temperature retrieved from the literature (Chiba et al., 2019). The $2p_{3/2}$ and $2p_{1/2}$ main peaks are accompanied by satellite peaks which can be described by configuration interaction calculations on a NiX_4 (X = S, Se) cluster model. In the cluster model, the ground state is given by a linear combination of d^8, d^9L and $d^{10}L^2$ configurations. The energy of d^9L relative to that of d^8 corresponds to the charge-transfer energy Δ. Then the energy of $d^{10}L^2$ is given by $2\Delta + U$ where U is the on-site Coulomb interaction energy between Ni 3d electrons. The transfer integrals between the Ni 3d and S 3p/Se 4p orbitals are expressed by Slater-Koster parameters (pdσ) and (pdπ). With Δ = −2.5 eV, U = 3.0 eV, and (pdσ) = -2.2 eV, the main and satellite peaks can be reproduced as shown by the solid curve in Figure 1D (Chiba et al., 2019). The good agreement with the cluster model calculation suggests that the effect of the Ni 2p core hole is strong enough for the Ni 3d electrons with the moderate d-d Coulomb interaction and the Se 4p electrons providing the strong p-d hybridization. The Δ and $2\Delta + U$ values are negative suggesting that the ground state is dominated by d^9L and $d^{10}L^2$ rather than d^8. Since the Ni 3d configuration is close to d^{10} and the 3d orbitals are almost fully occupied, the ground state would be compatible with the EI coupling between the Ni 3d hole and the Ta 5d electron. However, in the ground state obtained within the cluster model, the Ni 3d and Se 4p holes form a spin triplet state. It is rather complicated to create a nonmagnetic EI state starting from the spin triplet $d^9L/d^{10}L^2$ state (in the Ni chain) and the two Ta 5d electrons (in the Ta double chains) in the unit cell. Scattering theory analyses starting from the DFT band structure may be applied to describe the Ni 2p XPS. The Cu 2p XPS spectra of CuS and CuS_2 share the same problem (Goh et al., 2006; Laila et al., 2024) which should be examined in future.

Figure 1E shows XAS spectra of Ta_2NiSe_5 taken by total electron yield (TEY) with linearly polarized light of two different incident angles. The measurements were performed at 11ID-1 (SGM) of Canadian Light Source. The total energy resolution was 100 meV. The single crystals were cleaved under ultrahigh vacuum and measured without being exposed to the air. The base pressure of the XAS chamber was in the 10^{-8} Pa range. When the incidence angle is 0°, the polarization vector is parallel to the a-axis (chain direction). With the angle of 60°, the polarization vector has the out-of-plane component along the b-axis. The main absorption peak consists of two components A and B. In addition, the intense satellite peak (C) is observed at higher energy. The charge-transfer satellite may indicate that the Ni 2p XAS spectra should be analysed by the $NiSe_4$ cluster model. However, the polarization dependence of the main peak cannot be explained by the cluster model, and it is rather compatible with the orbital-resolved density of states obtained by DFT.

The Ta, Ni, and Se partial densities of states (PDOSs) calculated by generalized gradient approximation (GGA) are shown in Figure 1F, which is extracted from the literature (Takahashi and Mizokawa, 2022). The Ni 3d states are almost fully occupied indicating d^{10} configuration. The Ni 3d states are mixed into the conduction band through the strong Ni 3d-Se 4p and Se 4p-Ta 5d hybridization. The orbital-resolved Ni 3d PDOSs are shown in Figure 1G. The polarization dependence of the Ni 2p XAS spectra in Figure 1E is consistent with the orbital-resolved PDOS. The zx component is dominant around 0.5 eV above the Fermi level, consistent with the enhancement of peak A at the polarization angle of 60° (with out-of-plane polarization component). The xy component around 1.5 eV gains its intensity for the polarization angle of 0° (in-plane polarization) in agreement with the enhancement of peak B. While the Ni 2p XPS spectra are governed by the local charge-transfer process, the excited electrons in Ni 2p XAS are rather itinerant and can be described by the band picture. The intense satellite structure of Ni 2p XAS remains as a mystery. This situation is similar to CuS and CuS_2, where the Cu 3d orbitals are almost fully occupied and their Cu 2p XAS exhibits intense satellite structures (Goh et al., 2006; Laila et al., 2024). One possibility is that the Ni/Cu 3d component is strongly mixed with the conduction band (Ta 5d in Ta_2NiSe_5, S 3p in CuS or CuS_2) providing the spectral weight of the satellites. Another possibility is that the satellites are derived from the transitions from Ni/Cu 2p to Ni/Cu 4s. In future, this problem should be examined by more sophisticated theoretical calculations.

3 Angle-resolved RIXS of Ta_2NiSe_5

The angle-resolved RIXS data at the Ni 2p-3d edge of Ta_2NiSe_5 have been reported by Monney et al. (2020) which were performed at the advanced resonant spectroscopies (ADRESS) beamline (Strocov et al., 2010) of the Swiss Light Source, Paul Scherrer Institute, using the super-advanced x-ray emission spectrometer (SAXES) (Ghiringhelli et al., 2006). In this experiment, the incident and scattered x-rays are parallel to the a-b plane of Ta_2NiSe_5 as shown in Figure 2A. $\vec{Q}$ indicates the momentum transfer vector between the incident and scattered x-rays. Figure 2B shows the Ni 2p XAS taken with total fluorescence yield (TFY) at 30 K. The TFY result is basically consistent with the TEY one in Figure 1E. With the σ-polarization, the Ni 2p electron is mainly excited to the Ni 3d xy (in-plane) orbital corresponding to the absorption peak at 854.4 eV.

Figure 2C shows angle-resolved RIXS data for $\vec{Q} \sim \vec{0}$ which are taken at 30 K with σ-polarized incident x-ray with energies across the Ni 2p-3d edge (Monney et al., 2020). In the 2-dimensional map as a function of incident energy and energy loss, the intense resonant spectral weight is observed at about 854.4 eV and the non-resonant one disperses from 853 eV up to 860 eV. Figure 2D shows RIXS spectra acquired in the low incident energy region of Figure 2C. With the incident energy at the shoulder of 853 eV (Ni 3d zx state in Figure 1G), the zx band near the Fermi level is enhanced.

The resonant peak around energy loss of −0.4 eV can be assigned to the electron-hole excitations across the band gap which is created between the Ni 3d zx valence band and the Ta 5d conduction band through the strong Ni 3d-Se 4p and Se 4p-Ta 5d hybridization. The zx orbital anisotropy is consistent with the enhancement of the −0.4 eV peak at the XAS excitation around 853 eV which is enhanced with the polarization along z. The XAS excitation involves

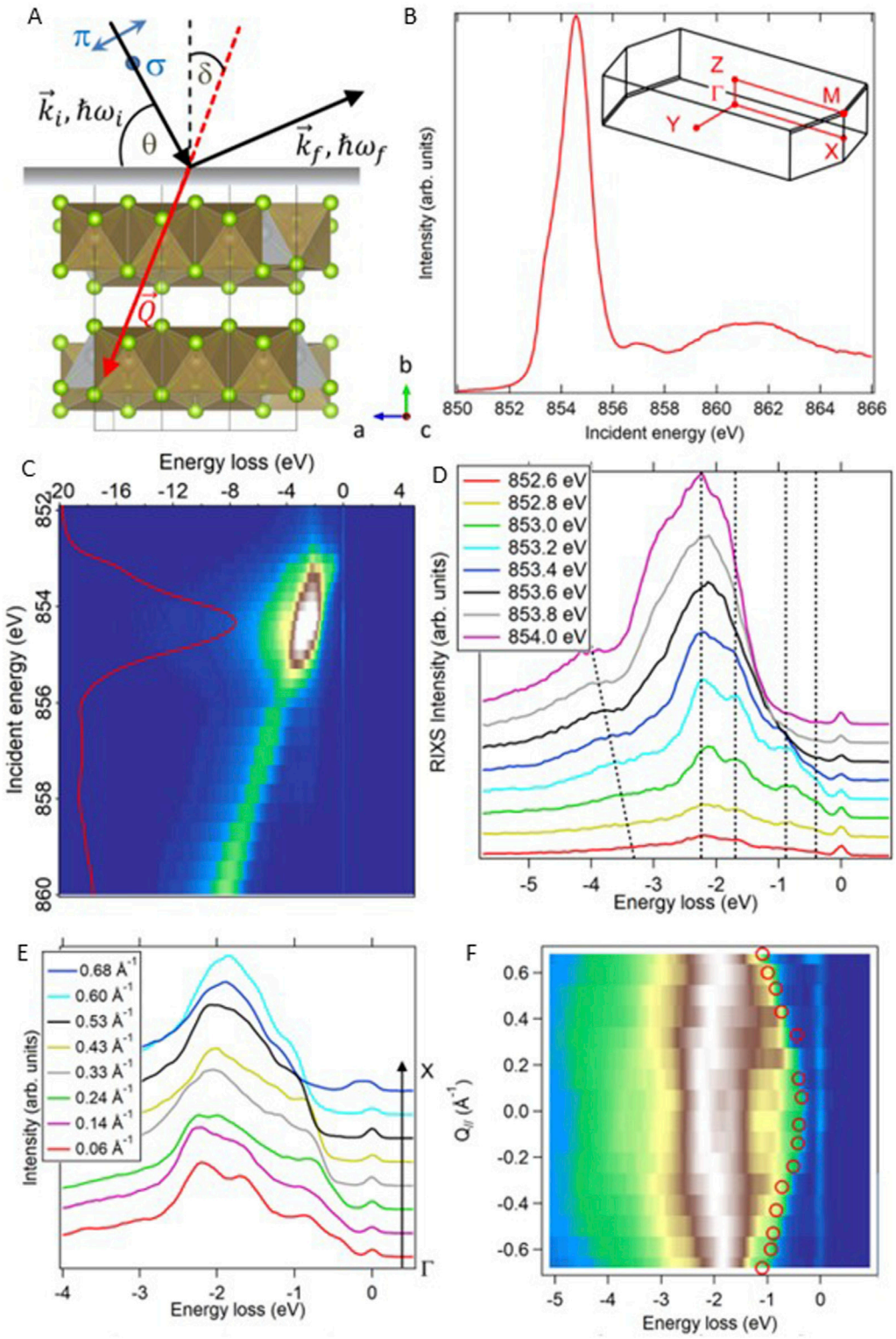

FIGURE 2
(A) Geometry of angle-resolved RIXS measurement. **(B)** Ni 2p XAS spectra (σ-polarization) of Ta_2NiSe_5. **(C)** RIXS map at 30 K as a function of incident energy and energy loss for the Ni 2p-3d excitation of Ta_2NiSe_5. **(D)** Ni 2p-3d RIXS spectra extracted from the low incident energy regions. **(E)** Angle-resolved Ni 2p-3d RIXS spectra along ΓX of Ta_2NiSe_5 taken with the σ-polarized x-ray of 853.3 eV **(F)** RIXS map as a function of in-plane momentum transfer $Q_{//}$ along ΓX and energy loss. The open circles indicate the edge of the electron-hole continuum extracted from the second derivative of the smoothed RIXS spectra. The figures are taken from the literature (Monney et al., 2020).

the Se 4p hole character which may play important roles to realize the exotic insulating state of Ta_2NiSe_5 deviating from the canonical EI state.

Figure 2E shows angle-resolved RIXS spectra as a function of in-plane momentum transfer $Q_{//}$ along ΓX taken at 30 K (Monney et al., 2020). Clear dispersions of the resonant peaks are observed, especially below 2 eV energy loss. At $Q_{//}$ = 0.06 $Å^{-1}$, the lowest energy excitation (leading edge) located around −0.4 eV corresponds to the electron-hole excitation with the zx orbital character in Figure 2D. The electron-hole excitation energy increases with $Q_{//}$. The $Q_{//}$ dependence of the electron-hole excitations is estimated from the position of the leading edge of the angle-resolved RIXS spectra in Figure 2E and is indicated by the open circles in Figure 2F. The dispersion of the electron-hole excitations can be fitted to a parabolic curve with effective mass of 1.7 m_e. Assuming that the edge of the electron-hole continuum is a convolution of the dispersions of the valence band top (Lower and higher bounds of the valence band effective mass are estimated to be 0.4 m_e and 0.8 m_e from ARPES (Wakisaka et al., 2012)) and the conduction band bottom, the effective mass of the conduction band is estimated to be between 1.3 m_e and 0.9 m_e (Monney et al., 2020). A new theoretical scheme is required to understand the RIXS of EIs which fails in between the localized and itinerant regimes. In this context, the DFT-based dynamical mean field theory (DMFT) (Hariki et al., 2020) and the density matrix normalization group technique (Zawadzki et al., 2023) will be a powerful tool to understand the EIs in a systematic manner.

4 Summary

When the transition-metal 3d orbitals are partially occupied, the transition-metal 2p-3d RIXS spectra are described by spin/charge/orbital excitations of the localized 3d electrons which gain their spectral weight through the strong 2p-3d interaction. On the other hand, the RIXS spectra of the EI candidates ($TiSe_2$ with d^0 and Ta_2NiSe_5 with d^{10}) are dominated by electron-hole excitations in the Bloch orbitals rather than the spin/charge/orbital excitations in the atomic orbitals. These observations indicate that the charge/orbital excitations of the EI candidates are basically described by the band picture. As for Ta_2NiSe_5, the orbital-resolved excitation becomes possible by tuning the incident energy in the two components of the main peak of Ni 2p XAS. With the excitation at peak A, the zx orbital component, which is located near the Fermi level and governs the gap formation, is enhanced. A low energy RIXS excitation less than 0.4 eV is observed near the elastic peak and can be assigned to the excitations from the valence band to the conduction band. The momentum dependence of the leading edge of the electron-hole excitations enables us to estimate the dispersion of the conduction band. It is still challenging to observe interplay between the phase mode and the phonon excitation predicted by the theoretical works for the EI candidates (Murakami et al., 2020) which can be elucidated in future with higher energy resolution. The present work suggests that localized charge-transfer excitations affect the electron-hole dynamics of Ta_2NiSe_5 in addition to the non-trivial electron-lattice coupling.

Author contributions

TM: Writing–original draft, Writing–review and editing. CM: Writing–original draft, Writing–review and editing.

Funding

The author(s) declare that financial support was received for the research, authorship, and/or publication of this article. CM acknowledges financial support by Swiss National Science Foundation (SNSF) Grant No. P00P2_170597.

Acknowledgments

The authors would like to thank Y. Wakisaka for the contributions of the XPS and XAS experiments on Ta_2NiSe_5, T. G. Regier for the support on the XAS measurements at CLS, M. Herzog and Prof. T. Schmitt for the collaboration on the angle-resolved RIXS measurements at SLS. They are grateful to Prof. N. Katayama, Prof. H. Sawa, Prof. M. Nohara, and Prof. H. Takagi for the long term collaborations on Ta_2NiSe_5 and related materials.

Conflict of interest

The authors declare that the research was conducted in the absence of any commercial or financial relationships that could be construed as a potential conflict of interest.

Publisher's note

References

Ament, L. J. P., van Veenendaal, M., Devereaux, T. P., Hill, J. P., and van den Brink, J. (2011). Resonant inelastic x-ray scattering studies of elementary excitations. *Rev. Mod. Phys.* 83, 705–767. doi:10.1103/RevModPhys.83.705

Baldini, E., Zong, A., Choi, D., Lee, C., Michael, M. H., Windgaetter, L., et al. (2023). The spontaneous symmetry breaking in Ta_2NiSe_5 is structural in nature. *PNAS* 120, e2221688120. doi:10.1073/pnas.2221688120

Bretscher, H. M., Andrich, P., Telang, P., Singh, A., Harnagea, L., Sood, A. K., et al. (2021). Ultrafast melting and recovery of collective order in the excitonic insulator Ta_2NiSe_5. *Nat. Commun.* 12, 1699. doi:10.1038/s41467-021-21929-3

Bronold, F. X., and Fehske, H. (2006). Possibility of an excitonic insulator at the semiconductor-semimetal transition. *Phys. Rev. B* 74, 165107. doi:10.1103/PhysRevB.74.165107

Bucher, B., Steiner, P., and Wachter, P. (1991). Excitonic insulator phase in $TmSe_{0.45}Te_{0.55}$. *Phys. Rev. Lett.* 67, 2717–2720. doi:10.1103/PhysRevLett.67.2717

Canadell, E., and Whangbo, W.-H. (1987). Metallic versus nonmetallic properties of ternary chalcogenides: tantalum metal selenide, Ta_2MSe_7 (M = nickel, platinum), and tantalum nickel chalcogenide, Ta_2NiX_5 (X = sulfide, selenide). *Inorg. Chem.* 26, 3974–3976. doi:10.1021/ic00271a003

Cercellier, H., Monney, C., Clerc, F., Battaglia, C., Despont, L., Garnier, M. G., et al. (2007). Evidence for an excitonic insulator phase in 1*T*–$TiSe_2$. *Phys. Rev. Lett.* 99, 146403. doi:10.1103/PhysRevLett.99.146403

Chiba, Y., Mitsuoka, T., Saini, N. L., Horiba, K., Kobayashi, M., Ono, K., et al. (2019). Valence-bond insulator in proximity to excitonic instability. *Phys. Rev. B* 100, 245129. doi:10.1103/PhysRevB.100.245129

DiSalvo, F. J., Chen, C. H., Fleming, R. M., Waszczak, J. V., Dunn, R. G., Sunshine, S. A., et al. (1986). Physical and structural properties of the new layered compounds Ta_2NiS_5 and Ta_2NiSe_5. *J. Less-Common Met.* 116, 51–61. doi:10.1016/0022-5088(86)90216-X

DiSalvo, F. J., Moncton, D. E., and Waszczak, J. V. (1976). Electronic properties and superlattice formation in the semimetal $TiSe_2$. *Phys. Rev. B* 14, 4321–4328. doi:10.1103/PhysRevB.14.4321

Ejima, S., Kaneko, T., Ohta, Y., and Fehske, H. (2014). Order, criticality, and excitations in the extended falicov-kimball model. *Phys. Rev. Lett.* 112, 026401. doi:10.1103/PhysRevLett.112.026401

Fukutani, K., Stania, R., Jung, J., Schwier, E. F., Shimada, K., Kwon, C. I., et al. (2019). Electrical tuning of the excitonic insulator ground state of Ta_2NiSe_5. *Phys. Rev. Lett.* 123, 206401. doi:10.1103/PhysRevLett.123.206401

Fukutani, K., Stania, R., Kwon, C. I., Kim, J. S., Kong, K. J., Kim, J., et al. (2021). Detecting photoelectrons from spontaneously formed excitons. *Nat. Phys.* 17, 1024. doi:10.1038/s41567-021-01289-x

Ghiringhelli, G., Piazzalunga, A., Dallera, C., Trezzi, G., Braicovich, L., Schmitt, T., et al. (2006). SAXES, a high resolution spectrometer for resonant x-ray emission in the 400-1600 eV energy range. *Rev. Sci. Instrum.* 77, 113108. doi:10.1063/1.2372731

Goh, S. W., Buckley, A. N., and Lamb, R. N. (2006). Copper(II) sulfide? *Miner. Eng.* 19, 204–208. doi:10.1016/j.mineng.2005.09.003

Halperin, B. I., and Rice, T. M. (1968). Possible anomalies at a semimetal-semiconductor transistion. *Rev. Mod. Phys.* 40, 755–766. doi:10.1103/RevModPhys.40.755

Haque, S. R. U., Michael, M. H., Zhu, J., Zhang, Y., Windgätter, L., Latini, S., et al. (2024). Terahertz parametric amplification as a reporter of exciton condensate dynamics. *Nat. Mater* 23, 796–802. doi:10.1038/s41563-023-01755-2

Hariki, A., Winder, M., Uozumi, T., and Kuneš, J. (2020). LDA + DMFT approach to resonant inelastic x-ray scattering in correlated materials. *Phys. Rev. B* 101, 115130. doi:10.1103/PhysRevB.101.115130

Hattori, M., Tomassucci, G., Hayashi, G., Okawa, M., Kopciuszynski, M., Barinov, A., et al. (2023). Robustness of excitonic coupling in Ta_2NiSe_5 against electronic inhomogeneity introduced by S substitution for Se. *Adv. Quantum Technol.* 6, 2300034. doi:10.1002/qute.202300034

He, Q., Que, X., Zhou, L., Isobe, M., Huang, D., and Takagi, H. (2021). Tunneling-tip-induced collapse of the charge gap in the excitonic insulator Ta_2NiSe_5. *Phys. Rev. Res.* 3, L032074. doi:10.1103/PhysRevResearch.3.L032074

Huang, J., Jiang, B., Yao, J., Yan, D., Lei, X., Gao, J., et al. (2024). Evidence for an excitonic insulator state in $Ta_2Pd_3Te_5$. *Phys. Rev. X* 14, 011046. doi:10.1103/PhysRevX.14.011046

Huber, M., Lin, Y., Marini, G., Moreschini, L., Jozwiak, C., Bostwick, A., et al. (2024). Ultrafast creation of a light-induced semimetallic state in strongly excited 1*T*-$TiSe_2$. *Sci. Adv.* 10, eadl4481. doi:10.1126/sciadv.adl4481

Ihle, D., Pfafferott, M., Burovski, E., Bronold, F. X., and Fehske, H. (2008). Bound state formation and the nature of the excitonic insulator phase in the extended Falicov-Kimball model. *Phys. Rev. B* 78, 193103. doi:10.1103/PhysRevB.78.193103

Jerome, D., Rice, T. M., and Kohn, W. (1967). Excitonic insulator. *Phys. Rev.* 158, 462–475. doi:10.1103/PhysRev.158.462

Jiang, Y., Mi, Y., Guo, J., Wang, Z., Zhang, N., Liu, B., et al. (2024). Multiple coherent amplitude modes and exciton–phonon coupling in quasi-one-dimensional excitonic insulator Ta_2NiSe_5. *Phys. Chem. Chem. Phys.* 26, 15417–15425. doi:10.1039/d4cp00261j

Kaneko, T., Toriyama, T., Konishi, T., and Ohta, Y. (2013). Orthorhombic-to-monoclinic phase transition of Ta_2NiSe_5 induced by the Bose-Einstein condensation of excitons. *Phys. Rev. B* 87, 035121. doi:10.1103/PhysRevB.87.035121

Kim, K., Kim, H., Kim, J., Kwon, C., Kim, J. S., and Kim, B. J. (2021). Direct observation of excitonic instability in Ta_2NiSe_5. *Nat. Commun.* 12, 1969. doi:10.1038/s41467-021-22133-z

Kogar, A., Rak, M. S., Vig, S., Husain, A. A., Flicker, F., Joe, Y. I., et al. (2017). Signatures of exciton condensation in a transition metal dichalcogenide. *Science* 358, 1314–1317. doi:10.1126/science.aam6432

Kotani, A., and Shin, S. (2001). Resonant inelastic x-ray scattering spectra for electrons in solids. *Rev. Mod. Phys.* 73, 203–246. doi:10.1103/RevModPhys.73.203

Laila, A. Z., Nguyen, T. L., Furui, R., Shelke, A., Chang, F.-H., Lin, H.-J., et al. (2024). Comparative study of a high-entropy metal disulfide and its parent compounds using x-ray absorption spectroscopy. *Phys. Rev. B* 109, 195129. doi:10.1103/PhysRevB.109.195129

Larkin, T. I., Dawson, R. D., Höppner, M., Takayama, T., Isobe, M., Mathis, Y.-L., et al. (2018). Infrared phonon spectra of quasi-one-dimensional Ta_2NiSe_5 and Ta_2NiS_5. *Phys. Rev. B* 98, 125113. doi:10.1103/PhysRevB.98.125113

Larkin, T. I., Yaresko, A. N., Pröpper, D., Kikoin, K. A., Lu, Y. F., Takayama, T., et al. (2017). Giant exciton Fano resonance in quasi-one-dimensional Ta_2NiSe_5. *Phys. Rev. B* 95, 195144. doi:10.1103/PhysRevB.95.195144

Lee, J., Kang, C.-J., Eom, M. J., Kim, J. S., Min, B. I., and Yeom, H. W. (2019). Strong interband interaction in the excitonic insulator phase of Ta_2NiSe_5. *Phys. Rev. B* 99, 075408. doi:10.1103/PhysRevB.99.075408

Liu, Q. M., Wu, D., Li, Z. A., Shi, L. Y., Wang, Z. X., Zhang, S. J., et al. (2021). Photoinduced multistage phase transitions in Ta_2NiSe_5. *Nat. Commun.* 12, 2050. doi:10.1038/s41467-021-22345-3

Lu, H., Gauthier, A., Hepting, M., Tremsin, A. S., Reid, A. H., Kirchmann, P. S., et al. (2020). Time-resolved RIXS experiment with pulse-by-pulse parallel readout data collection using X-ray free electron laser. *Sci. Rep.* 10, 22226. doi:10.1038/s41598-020-79210-4

Lu, Y. F., Kono, H., Larkin, T. I., Rost, A. W., Takayama, T., Boris, A. V., et al. (2017). Zero-gap semiconductor to excitonic insulator transition in Ta_2NiSe_5. *Nat. Commun.* 8, 14408. doi:10.1038/ncomms14408

Matsubayashi, K., Okamura, H., Mizokawa, T., Katayama, N., Nakano, A., Sawa, H., et al. (2021). Hybridization-gap formation and superconductivity in the pressure-induced semimetallic phase of the excitonic insulator Ta_2NiSe_5. *J. Phys. Soc. Jpn.* 90, 074706. doi:10.7566/JPSJ.90.074706

Mazza, G., Rösner, M., Windgätter, L., Latini, S., Hubener, H., Millis, A. J., et al. (2020). Nature of symmetry breaking at the excitonic insulator transition: Ta_2NiSe_5. *Phys. Rev. Lett.* 124, 197601. doi:10.1103/PhysRevLett.124.197601

Mitsuoka, T., Suzuki, T., Takagi, H., Katayama, N., Sawa, H., Nohara, M., et al. (2020). Photoinduced phase transition from excitonic insulator to semimetal-like state in $Ta_2Ni_{1-x}Co_xSe_5$ (x = 0.10). *J. Phys. Soc. Jpn.* 89, 124703. doi:10.7566/JPSJ.89.124703

Miyamoto, T., Mizui, M., Takamura, N., Hirata, J., Yamakawa, H., Morimoto, T., et al. (2022). Charge and lattice dynamics in excitonic insulator Ta_2NiSe_5 investigated using ultrafast Reflection spectroscopy. *J. Phys. Soc. Jpn.* 91, 023701. doi:10.7566/JPSJ.91.023701

Monney, C., Cercellier, H., Clerc, F., Battaglia, C., Schwier, E. F., Didiot, C., et al. (2009). Spontaneous exciton condensation in 1*T*-$TiSe_2$: BCS-like approach. *Phys. Rev. B* 79, 045116. doi:10.1103/PhysRevB.79.045116

Monney, C., Herzog, M., Pulkkinen, A., Huang, Y., Pelliciari, J., Olalde-Velasco, P., et al. (2020). Mapping the unoccupied state dispersions in Ta_2NiSe_5 with resonant inelastic x-ray scattering. *Phys. Rev. B* 102, 085148. doi:10.1103/PhysRevB.102.085148

Monney, C., Monney, G., Aebi, P., and Beck, H. (2012a). Electron-hole fluctuation phase in 1*T*-$TiSe_2$. *Phys. Rev. B* 85, 235150. doi:10.1103/PhysRevB.85.235150

Monney, C., Puppin, M., Nicholson, C. W., Hoesch, M., Chapman, R. T., Springate, E., et al. (2016). Revealing the role of electrons and phonons in the ultrafast recovery of charge density wave correlations in 1*T*–$TiSe_2$. *Phys. Rev. B* 94, 165165. doi:10.1103/PhysRevB.94.165165

Monney, C., Schwier, E. F., Garnier, M. G., Mariotti, N., Didiot, C., Beck, H., et al. (2010). Temperature-dependent photoemission on 1*T*-$TiSe_2$: interpretation within the exciton condensate phase model. *Phys. Rev. B* 81, 155104. doi:10.1103/PhysRevB.81.155104

Monney, C., Zhou, K. J., Cercellier, H., Vydrova, Z., Garnier, M. G., Monney, G., et al. (2012b). Mapping of electron-hole excitations in the charge-density-wave system 1*T*–$TiSe_2$ using resonant inelastic X-ray scattering. *Phys. Rev. Lett.* 109, 047401. doi:10.1103/PhysRevLett.109.047401

Mor, S., Herzog, M., Golež, D., Werner, P., Eckstein, M., Katayama, N., et al. (2017). Ultrafast electronic band gap control in an excitonic insulator. *Phys. Rev. Lett.* 119, 086401. doi:10.1103/PhysRevLett.119.086401

Mor, S., Herzog, M., Monney, C., and Stähler, J. (2022). Ultrafast charge carrier and exciton dynamics in an excitonic insulator probed by time-resolved photoemission spectroscopy. *Prog. Surf. Sci.* 97, 100679. doi:10.1016/j.progsurf.2022.100679

Mor, S., Herzog, M., Noack, J., Katayama, N., Nohara, M., Takagi, H., et al. (2018). Inhibition of the photoinduced structural phase transition in the excitonic insulator Ta_2NiSe_5. *Phys. Rev. B* 97, 115154. doi:10.1103/PhysRevB.97.115154

Mott, N. F. (1961). The transition to the metallic state. *Phil. Mag.* 6, 287–309. doi:10.1080/14786436108243318

Murakami, Y., Golez, D., Kaneko, T., Koga, A., Millis, A. J., and Werner, P. (2020). Collective modes in excitonic insulators: effects of electron-phonon coupling and signatures in the optical response. *Phys. Rev. B* 101, 195118. doi:10.1103/PhysRevB.101.195118

Nakano, A., Hasegawa, T., Tamura, S., Katayama, N., Tsutsui, S., and Sawa, H. (2018). Antiferroelectric distortion with anomalous phonon softening in the excitonic insulator Ta_2NiSe_5. *Phys. Rev. B* 98, 045139. doi:10.1103/PhysRevB.98.045139

Neuenschwander, J., and Wachter, P. (1990). Pressure-driven semiconductor-metal transition in intermediate-valence $TmSe_{1-x}Te_x$ and the concept of an excitonic insulator. *Phys. Rev. B* 41, 12693–12709. doi:10.1103/PhysRevB.41.12693

Okamura, H., Mizokawa, T., Miki, K., Matsui, Y., Noguchi, N., Katayama, N., et al. (2023). Pressure suppression of the excitonic insulator state in Ta_2NiSe_5 observed by optical conductivity. *Phys. Rev. B* 107, 045141. doi:10.1103/PhysRevB.107.045141

Okazaki, K., Ogawa, Y., Suzuki, T., Yamamoto, T., Someya, T., Michimae, S., et al. (2018). Photo-induced semimetallic states realised in electron–hole coupled insulators. *Nat. Commun.* 9, 4322. doi:10.1038/s41467-018-06801-1

Phan, V.-N., Becker, K. W., and Fehske, H. (2010). Spectral signatures of the BCS-BEC crossover in the excitonic insulator phase of the extended Falicov-Kimball model. *Phys. Rev. B* 81, 205117. doi:10.1103/PhysRevB.81.205117

Pillo, Th., Hayoz, J., Berger, H., Lévy, F., Schlapbach, L., and Aebi, P. (2000). Photoemission of bands above the Fermi level: the excitonic insulator phase transition in 1*T*–$TiSe_2$. *Phys. Rev. B* 61, 16213–16222. doi:10.1103/PhysRevB.61.16213

Qian, D., Hsieh, D., Wray, L., Morosan, E., Wang, N. L., Xia, Y., et al. (2007). Emergence of fermi pockets in a new excitonic charge-density-wave melted superconductor. *Phys. Rev. Lett.* 98, 117007. doi:10.1103/PhysRevLett.98.117007

Rohwer, T., Hellmann, S., Wiesenmayer, M., Sohrt, C., Stange, A., Slomski, B., et al. (2011). Collapse of long-range charge order tracked by time-resolved photoemission at high momenta. *Nature* 471, 490–493. doi:10.1038/nature09829

Rossnagel, K., Kipp, L., and Skibowski, M. (2002). Charge-density-wave phase transition in 1T-TiSe2: excitonic insulator versus band-type Jahn-Teller mechanism. *Phys. Rev. B* 65, 235101. doi:10.1103/PhysRevB.65.235101

Saha, T., Golež, D., Ninno, G. D., Mravlje, J., Murakami, Y., Ressel, B., et al. (2021). Photoinduced phase transition and associated timescales in the excitonic insulator Ta_2NiSe_5. *Phys. Rev. B* 103, 144304. doi:10.1103/PhysRevB.103.144304

Seki, K., Eder, R., and Ohta, Y. (2011). BCS-BEC crossover in the extended Falicov-Kimball model: variational cluster approach. *Phys. Rev. B* 84, 245106. doi:10.1103/PhysRevB.84.245106

Seki, K., Wakisaka, Y., Kaneko, T., Toriyama, T., Konishi, T., Sudayama, T., et al. (2014). Excitonic Bose-Einstein condensation in Ta_2NiSe_5 above room temperature. *Phys. Rev. B* 90, 155116. doi:10.1103/PhysRevB.90.155116

Strocov, V. N., Schmitt, T., Flechsig, U., Schmidt, T., Imhof, A., Chen, Q., et al. (2010). High-resolution soft X-ray beamline ADRESS at the Swiss Light Source for resonant inelastic X-ray scattering and angle-resolved photoelectron spectroscopies. *J. Synchrotron Radiat.* 17, 631–643. doi:10.1107/S0909049510019862

Sunshine, S. A., and Ibers, J. A. (1985). Structure and physical properties of the new layered ternary chalcogenides tantalum nickel sulfide Ta_2NiS_5 and tantalum nickel selenide Ta_2NiSe_5. *Inorg. Chem.* 24, 3611–3614. doi:10.1021/ic00216a027

Suzuki, T., Shinohara, Y., Lu, Y. F., Watanabe, M., Xu, J., Ishikawa, K. L., et al. (2021). Detecting electron-phonon coupling during photoinduced phase transition. *Phys. Rev. B* 103, L121105. doi:10.1103/PhysRevB.103.L121105

Takahashi, Y., and Mizokawa, T. (2022). Impact of Co or Cu substitution for Ni on the electronic structure of Ta_2NiSe_5 studied by band structure calculations. *J. Phys. Soc. Jpn.* 91, 074714. doi:10.7566/JPSJ.91.074714

Takahashi, Y., Suzuki, T., Hattori, M., Okawa, M., Takagi, H., Katayama, N., et al. (2023). Temporal evolution and fluence dependence of band structure in photoexcited $Ta_2Ni_{0.9}Co_{0.1}Se_5$ probed by time- and angle-resolved photoemission spectroscopy. *J. Phys. Soc. Jpn.* 92, 064706. doi:10.7566/jpsj.92.064706

Takubo, K., Nambu, Y., Nakatsuji, S., Wakisaka, Y., Sudayama, T., Fournier, D., et al. (2010). Separation between low-energy hole dynamics and spin dynamics in a frustrated magnet. *Phys. Rev. Lett.* 104, 226404. doi:10.1103/PhysRevLett.104.226404

Volkov, P. A., Ye, M., Lohani, H., Feldman, I., Kanigel, A., and Blumberg, G. (2021). Failed excitonic quantum phase transition in $Ta_2Ni(Se_{1-x}S_x)_5$. *Phys. Rev. B* 104, L241103. doi:10.1103/PhysRevB.104.L241103

Wachter, P., Bucher, B., and Malar, J. (2004). Possibility of a superfluid phase in a Bose condensed excitonic state. *Phys. Rev. B* 69, 094502. doi:10.1103/PhysRevB.69.094502

Wakisaka, Y., Sudayama, T., Takubo, K., Mizokawa, T., Arita, M., Namatame, H., et al. (2009). Excitonic insulator state in Ta_2NiSe_5 probed by photoemission spectroscopy. *Phys. Rev. Lett.* 103, 026402. doi:10.1103/PhysRevLett.103.026402

Wakisaka, Y., Sudayama, T., Takubo, K., Mizokawa, T., Saini, N. L., Arita, M., et al. (2012). Photoemission spectroscopy of Ta_2NiSe_5. *J. Supercond. Nov. Magn.* 25, 1231–1234. doi:10.1007/s10948-012-1526-0

Watson, M. D., Markovic, I., Morales, E. A., LeFevre, P., Merz, M., Haghighirad, A. A., et al. (2020). Band hybridization at the semimetal-semiconductor transition of Ta_2NiSe_5 enabled by mirror-symmetry breaking. *Phys. Rev. Res.* 2, 013236. doi:10.1103/PhysRevResearch.2.013236

Werdehausen, D., Takayama, T., Höppner, M., Albrecht, G., Rost, A. W., Lu, Y. F., et al. (2018). Coherent order parameter oscillations in the ground state of the excitonic insulator Ta_2NiSe_5. *Sci. Adv.* 4, eaap8652. doi:10.1126/sciadv.aap8652

Ye, M., Volkov, P. A., Lohani, H., Feldman, I., Kim, M., Kanigel, A., et al. (2021). Lattice dynamics of the excitonic insulator $Ta_2Ni(Se_{1-x}S_x)_5$. *Phys. Rev. B* 104, 045102. doi:10.1103/PhysRevB.104.045102

Zawadzki, K., Nocera, A., and Feiguin, A. E. (2023). A time-dependent momentum-resolved scattering approach to core-level spectroscopies. *SciPost Phys.* 15, 166. doi:10.21468/SciPostPhys.15.4.166

Zhang, P., Dong, Y., Yan, D., Jiang, B., Yang, T., Li, J., et al. (2024). Spontaneous gap opening and potential excitonic states in an ideal Dirac semimetal $Ta_2Pd_3Te_5$. *Phys. Rev. X* 14, 011047. doi:10.1103/PhysRevX.14.011047

Zhao, J. F., Ou, H. W., Wu, G., Xie, B. P., Zhang, Y., Shen, D. W., et al. (2007). Evolution of the electronic structure of 1*T*–Cu_xTiSe_2. *Phys. Rev. Lett.* 99, 146401. doi:10.1103/PhysRevLett.99.146401

Zittartz, J. (1967). Anisotropy effects in the excitonic insulator. *Phys. Rev.* 162, 752–758. doi:10.1103/PhysRev.162.752